Colloids and Surfaces B: Biointerfaces 139 (2016) 25–32

Contents lists available at ScienceDirect

Colloids and Surfaces B: Biointerfaces

journal homepage: www.elsevier.com/locate/colsurfb

Reversing the peptide sequence impacts on molecular surface behaviour

Ernesto E. Ambroggio[a,*], Benjamín Caruso[a,1], Marcos A. Villarreal[b,1], Vincent Raussens[c], Gerardo D. Fidelio[a]

[a] CIQUIBIC, CONICET, Departamento de Química Biológica, Facultad de Ciencias Químicas, Universidad Nacional de Córdoba, Argentina
[b] Instituto de Investigaciones en Físico-Química de Córdoba (INFIQC), CONICET, Departamento de Matemática y Física, Facultad de Ciencias Químicas, Universidad Nacional de Córdoba, Ciudad Universitaria, Córdoba, Argentina
[c] Centre for Structural Biology and Bioinformatics, Laboratory for Structure and Function of Biological Membranes, Universit é Libre de Bruxelles, CP 206/02, Blvd. du Triomphe, B-1050 Brussels, Belgium

ARTICLE INFO

Article history:
Received 17 September 2015
Received in revised form
20 November 2015
Accepted 2 December 2015
Available online 4 December 2015

Keywords:
Peptide Langmuir monolayer stability
Peptide retro-isomers
Peptide adsorption/penetration into interfaces
Peptide/membrane interaction
Peptide Langmuir rheology monolayer

ABSTRACT

The protein's primary structure has all the information for specific protein/peptide folding and, in many cases, can define specific amphiphilic regions along molecules that are important for interaction with membranes. In order to shed light on how peptide sequence is important for the surface properties of amphiphilic peptides, we designed three pairs of peptides with the following characteristics: (1) all molecules have the same hydrophobic residues; (2) the couples differ from each other in their hydrophilic amino acids: positively, negatively and non-charged; (3) each pair has the same residues (same global molecular hydrophobicity) but the primary structure is reversed in comparison to its partner (retro-isomer), giving a molecule with a hydrophilic N or C-terminus and a hydrophobic C or N-terminus. Using the Langmuir monolayer approach, we observed that sequence reversal has a central role in the lateral stability of peptide monolayers, in the ability of the molecules to partition into the air–water interface and in the rheological properties of peptide films, whereas the peptide's secondary structure, determined by ATR-FTIR, was the same for all peptides. Reversing the sequence also gives a differential way of peptide/lipid interaction when peptides are in the presence of POPC lipid bilayers. Our results show how sequence inversion confers a distinctive peptide surface behaviour and lipid interaction for molecules with a similar structure.

1. Introduction

At cellular membrane level, amphiphilic peptides can perform different activities or be involved in several processes. For example, many proteins interact with membranes through amphiphilic alpha-helical peptides [1–4]. Several amphipathic peptides, like the antibiotic melittin and maculatin (among others) or cytotoxic peptides, such as beta-amyloids, alpha-synuclein, etc. when interacting with membranes, present toxic activity with different membrane-damaging modes [5–9] or are able to sense/stabilise membrane curvature as is the case of, for example, the amphiphilic peptides of the BAR proteins, the ALPS motif of ArfGAP1 and others [10–14]. In addition, protein transport through membranes is mediated, in many cases, by a N-terminal signal sequence peptide (SSP) that interacts with interfaces containing the translocation machinery [15,16].

The general structure of a SSP consists of a positively charged N-terminal region (n-region), followed by a hydrophobic core region (h-region) before the C-terminal region (c-region) and a cleavage site [17]. Rapoport's laboratory has shown that there is a close interaction between SSPs and the lipids of the directed membrane [18]. Once at the membrane, the signal sequence peptides are cleaved off by a signal peptidase [18,19]. This shows the importance of a perfect membrane/SSP interaction for correct protein transport, where the insertion of the peptide maintains the integrity of the lipid bilayer from insertion until recycling, an important biological aspect of SSPs reviewed by Rapoport [18]. However, apart from information of the translocation machinery and the lipid interaction of this type of peptides at membrane level, neither the role

* Corresponding author at: CIQUIBIC, CONICET, Departamento de Química Biológica, Fac. Cs. Qcas Universidad Nacional de Córdoba. Haya de la Torre y Medina Allende, Ciudad Universitaria, X5000HUA Córdoba, Argentina. Fax: +54 3515353855.
E-mail address: ambroggioernesto@yahoo.com (E.E. Ambroggio).
[1] These authors contributed equally.

http://dx.doi.org/10.1016/j.colsurfb.2015.12.008
0927-7765/

Table 1
Amino acid sequence of the N-acetylated (Ac-) and C-amidated (-NH2) peptides designed for the interfacial studies performed in this work.

Peptide name	Sequence
KL	KKGWLLLLL
LK	LLLLLLWGKK
EL	EEGWLLLLL
LE	LLLLLLWGEE
SL	SSGWLLLLL
LS	LLLLLLWGSS

of membrane lipids nor the surface properties of signal sequences has been finely studied. We recently showed that SSPs form insoluble monolayers with high stability against lateral compression, a lipid-like property for this type of peptides to support high lateral pressures when embedded inside membranes [20].

The aim of this work is to understand the function of a specific molecular configuration of peptides in the interfacial properties of molecules. To achieve this, it is necessary to study peptides with a rational design of their amino acid sequence. Therefore, based on what is known of the configuration of SSPs, we synthesised three pairs of peptides (Table 1) and analysed their surface behaviour and rheology at the air–water interface and their association with lipid interfaces. Here we show that peptides that present hydrophilic residues in the N-terminal region (N-philic peptides) have the highest surface stability against lateral compression, a better ability to partition into the air–water interface and an enhanced capacity to penetrate lipid interfaces, in comparison to their retro-isomeric [21] homologue molecules that have hydrophilic amino acids at the C-terminus (C-philic peptides). The data show how a specific molecular configuration has evolved to reach the perfect biological design of proteins and peptides for precise interaction with membrane interfaces.

2. Material and methods

2.1. Reagents

Peptides were purchased from Peptide 2.0 (Chantilly, VA, USA). NaCl was from J.T. Baker (Center Valley, PA, USA) and DMSO from Merck (Darmstadt, Germany). Lipids and NBD-PE (1,2-dioleoyl-*sn*-glycero-3-phosphoethanolamine-*N*-(7-nitro-2-1,3-benzoxadiazol-4-yl)) were obtained from Avanti Polar lipids, Inc. (Alabaster, AL, USA).

2.2. Langmuir and Gibbs monolayers

Langmuir monolayer experiments of pure peptides were performed on an 80 cm^2 homemade Teflon trough containing 75 ml of NaCl 145 mM. Peptides were dissolved in DMSO to a final concentration of 0.5–1.5 mM and directly spread onto the air–NaCl 145 mM (air–aqueous) interface with a Hamilton syringe. The surface pressure (measured employing the Wilhelmy method via platinised-Pt plate) and the area enclosing the monolayer were automatically registered (Monofilmmeter with Film Lift, Mayer-Feintechnik, Göttingen, Germany).

Adsorption experiments (Gibbs peptide monolayer formation) were performed, injecting the peptides from their DMSO solution into 18 ml of NaCl 145 mM contained in an 18 cm^2 homemade trough under continuous stirring.

Peptide penetration into the POPC monolayers was carried out by spreading the lipid onto the air–aqueous interface (18 cm^2 surface area trough) until reaching a stable 20 mN/m lateral pressure. Then, as in the adsorption experiments, the peptides were injected from a DMSO solution into 18 ml of NaCl 145 mM under constant stirring. The change of lateral pressure due to peptide penetration into the lipid monolayers was continuously monitored. Control experiments were performed with only DMSO, and showed no effect of this solvent.

2.3. Monolayer rheology

Anisotropic monolayer area oscillation experiments were carried out as described previously [22,23] and following the procedures described in detail by Cicuta and Terentjev [24]. Briefly, the peptide Langmuir film was isometrically compressed with two barriers (i.e. anisotropically) up to the desired lateral pressure. Then, sinusoidal area perturbations by compression–expansion cycles were performed while measuring both the surface pressure and the phase shift between the tension and the surface area signals (see Fig. S3 in Supplementary material). Since the deformation created by the moving barrier is uniaxial, the surface pressure is a superposition of well-defined dilatation and shear moduli. Therefore, taking into account that the interfacial tension is a tensor quantity, the measured values depend on the direction of the axis along which the stress acts [25]. The calculations used to obtain the rheological parameters are explained in Supplementary material section (Section 2.1 and Fig. S3). In addition, we measured the diffusion of latex beads in a pure peptide interface in order to account for the microrheological properties of the film (where the oscillating technique has less resolution) (see Supplementary material, Section 2.2 and Fig. S4).

2.4. LUVs preparation and FRET measurements

Large unilamellar vesicles (LUVs) were prepared by the extrusion method [26]. Concisely, multilamellar vesicles (MLVs) were produced by dispersing dry lipid in 145 mM NaCl with vortex mixing and 5 cycles of freezing (liquid nitrogen)/thawing (37 °C). This suspension of MLVs was manually extruded through a 100 nm polycarbonate filter by using a mini-Extruder set (Avanti Polar Lipids; Alabaster, AL, US). Monodisperse LUVs of around 90–100 nm in size were obtained after extrusion.

In order to monitor peptide binding to LUVs, we used a classical tryptophan-NBD fluorescence energy transfer assay (FRET) [27]. For our experiments, POPC LUVs doped with 1% NBD-PE (1,2-dioleoyl-*sn*-glycero-3-phosphoethanolamine-*N*-(7-nitro-2-1,3-benzoxadiazol-4-yl)) were used at a final concentration of 1.5 mM. The peptides (DMSO solution) were injected into a cylindrical fluorescence cuvette (experimental volume: 400 μl; 4 μM final peptide concentration) containing the NBD-LUVs under continuous stirring. Before and after peptide injection, the FRET was monitored, detecting NBD emission at 536 nm wavelength when tryptophan was excited at 280 nm. Control experiments were performed with DMSO only, and showed no effect of this solvent.

2.5. ATR-FTIR

IR spectra were recorded on an Equinox 55 IR spectrophotometer (Bruker Optics) equipped with a single reflection diamond ATR accessory (Golden Gate, Specac). The spectrometer was continuously purged with dried air. A total of 256 accumulations were performed to improve the signal/noise ratio. Spectra were recorded at 21 °C using a resolution of 2 cm^{-1}. The peptide sample (1.5–5 μl) was spread onto the diamond crystal surface and excess solvent (DMSO, water, or DMSO:Chloroform:Methanol) was removed under nitrogen flow.

For the secondary structure analysis, the water vapour and side chain contributions were subtracted and then the spectra were baseline corrected and normalised for equal area between 1700 and 1500 cm^{-1}. All spectra were deconvoluted using a Lorentzian deconvolution factor with a full width at the half maximum of

20 cm^{-1} and a Gaussian apodisation factor with a full width at the half maximum of 13.33 cm^{-1} to obtain a resolution enhancement factor $K = 1.5$. The bands identified in the deconvoluted spectra were used for curve fitting of the original ($K = 1$) spectra using Gaussian/Lorentzian bands [28].

3. Results

3.1. Peptide design

As described before, the general properties of a sequence of a SSP consist of a positively charged N-terminal region, followed by a hydrophobic core region before the C-terminal region (c-region) [17]. Based on this sequence consensus, we first designed three peptides (N-acetylated and C-amidated) that mimic the first half of the SSPs, but with different properties at the N-terminus. Their N-terminal region is hydrophilic ("N-philic peptides"), and they are positively or negatively charged or neutral (Table 1, peptides KL, EL and SL respectively).

In addition, we introduced a glycine to allow mobility at the interface between this hydrophilic N-region and the hydrophobic C-terminus region formed by WL_6. This design allows us to test how N-philic peptides with different hydrophilic residues behave at the air–aqueous interface and what type of structure they adopt. This attempts to tackle, in interfacial terms, why a positive N-terminus is necessary for SSPs to interact with membranes and whether a general hydrophilic region is needed. Next, we planned molecules that have the same residues as the above-mentioned peptides but with their sequence reversed (retro-isomer [21]) with respect to their homologue (Table 1, peptides LK, LE and LS), giving a peptide with a hydrophilic C-region (C-philic). With this configuration, we were able to compare the surface behaviour, the interaction with lipids and the secondary structure of two molecules that have the same hydrophobicity and amino-acid composition but the opposite primary structure. Again, differential results will explain not only why a specific design evolved in cells, but also why others were ruled out. It should be noted that the sequences used here represent one half of an entire SSP, because only the first layer of a hypothetic lipid bilayer is represented in the Langmuir studies.

3.2. Peptide Langmuir monolayers

3.2.1. Lateral compression isotherms of pure peptide monolayers

We first evaluated the lateral interfacial stability of the amphiphilic peptides by generating an insoluble peptide film at the air–NaCl 145 mM interface ("air–aqueous interface") and then laterally compressing the monolayer. The higher the collapse pressure of the film, the higher its monolayer stability [29]. Fig. 1 shows the compression isotherms (expressed as the lateral pressure of the film as a function of the molecular area) for the three pairs of peptides. The differences between N-philic and C-philic are clear-cut: monolayers of N-philic peptides have notably higher collapse pressures than monolayers of C-philic peptides (see inserted table in Fig. 1). The limiting molecular areas (molecular area at the collapse pressure) of the peptide pairs show slight differences, with KL/LK > EL/LE > SL/LS. These differences in the area at maximal packing correlate with the differences of the volume of the hydrophilic residues [30].

In parallel, we performed molecular dynamic simulations of peptide monolayers packed up to 1 nm^2 (see Supplementary material and Fig. S1). Confirming the experimental data, the reduction of the aqueous surface tension was higher for N-philic peptide monolayers than for C-philic (Fig. S2). This is important as it shows how SSPs are able to bear high lateral pressures when inserted in membranes because of their initial half of the peptide, where this N-philic configuration is the one that resists high lateral packing.

Table 2
Rheological characterization obtained from the anisotropic area oscillation of peptide monolayers. Dilatational (εí) and shear (G í) elastic moduli of pure peptide Langmuir monolayers. The data shown is the average of more than two independent experiments.

Peptide	ε' (mN/m)	G' (mN/m)
KL	110.2	30.6
LK	89.4	4.7
EL	112.8	40.5
LE	108.7	26.6
SL	113.8	20.5
LS	113.8	19.6

3.3. Rheology of pure peptide Langmuir monolayers

The anisotropic area oscillation experiment allows the elastic and viscous components of both the dilatational and shear moduli of protein monolayers to be assessed [24]. Our aim was to understand whether the two different peptide configurations, N- and C-philic, develop films with specific rheological properties. All the molecules studied here form elastic films, presenting both dilatational (ε') and shear (G') contributions (Table 2), which is indicative of the presence of a network [24,31]. For the charged peptides, there is a clear difference between the retro-isomers, where the shear modulus was found to be higher for the N-philic peptides. All of these peptides exhibit negligible dilatational (ε'') and shear (G'') viscosities (in relation to the elasticity detected with this method). As the anisotropic oscillation method requires oscillation at a minimal critical surface pressure, we used a microrheological technique, a more sensitive method that allows qualitative measurement of the shear response of each peptide monolayer. This technique is based on the tracking of latex spheres that diffuse on the monolayer (Supplementary material, Fig. S4). In our experiments, bead diffusion was very slow for all of the evaluated surface lateral pressures. This was observed even at the lift-off surface pressure (1–2 mN/m; Fig. S4). This means that the peptides form films with a high shear stress response, comparable to that observed in the Aβ1-40/42 peptides and in contrast with the α-helix melittin [23] (Caruso et al., unpublished results). From these analyses, it is now evident why a charged N-philic configuration is probably important for SSPs, since films of these peptides show a high shear modulus allowing these molecules to respond to high lateral pressure fluctuations when forming a film.

3.4. Peptide incorporation into the air–water interface

Since there was a marked difference between monolayers of the N-philic and C-philic peptides in terms of lateral stability and rheology, we next wanted to know whether both types of peptides had differences in terms of spontaneous adsorption into the air–aqueous interface. To test this, we injected each peptide into the aqueous phase and monitored the change in lateral pressure due to the adsorption of molecules into the interface (Fig. 2). Significantly, the N-philic peptides, KL and EL, showed a higher capacity to partition into the interface than their C-philic homologues (LK or LE, respectively). On the other hand, at the same concentration (and at concentrations doubling those for KL, LK, EL and LE; data not shown), SL and LS did not self-incorporate into the air–aqueous interface. In line with the above results, N-philic peptides have a higher thermodynamic tendency than C-philic peptides to partition into the air–water interface, which shows the importance of this configuration for optimal interaction with and insertion in biological membranes.

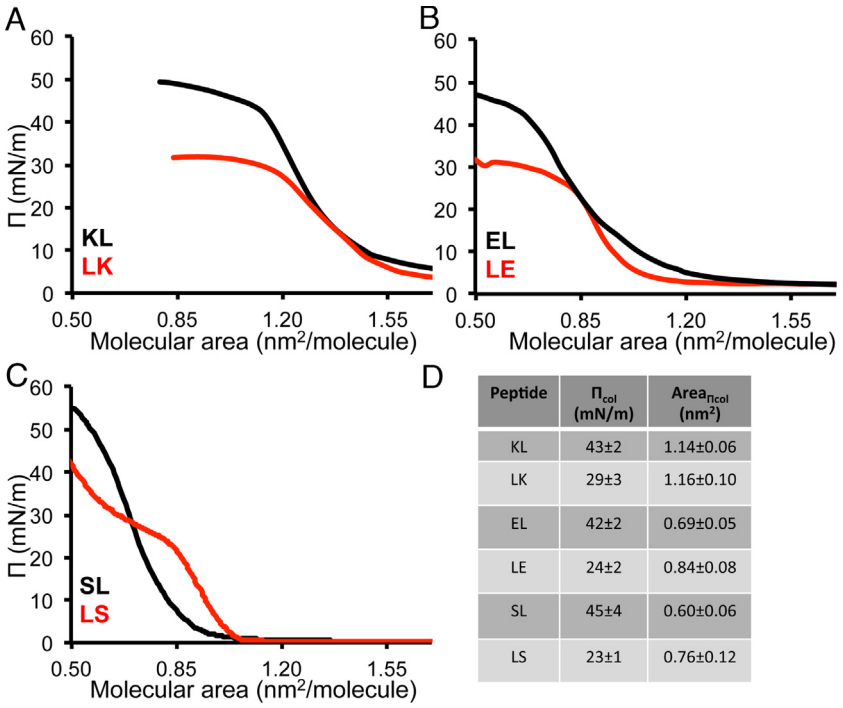

Peptide	Π_{col} (mN/m)	$Area_{\Pi col}$ (nm^2)
KL	43±2	1.14±0.06
LK	29±3	1.16±0.10
EL	42±2	0.69±0.05
LE	24±2	0.84±0.08
SL	45±4	0.60±0.06
LS	23±1	0.76±0.12

Fig. 1. Pure peptide monolayers. Lateral surface pressure (II) vs. molecular area isotherms of KL and LK (A), EL and LE (B) and SL and LS peptides (C). Black lines: N-philic peptides. Red lines: C-philic peptides. (D) Table with a summary of the lateral stability of the different peptide films (collapse pressure, II_{col}) and the molecular area at this point. II_{col} was determined by the slope change (derivative) of the compression isotherm curve after lift-off. At this point the molecular area is obtained. The data shown is the result of the average of three independent experiments. (For interpretation of the references to colour in this figure legend, the reader is referred to the web version of this article.)

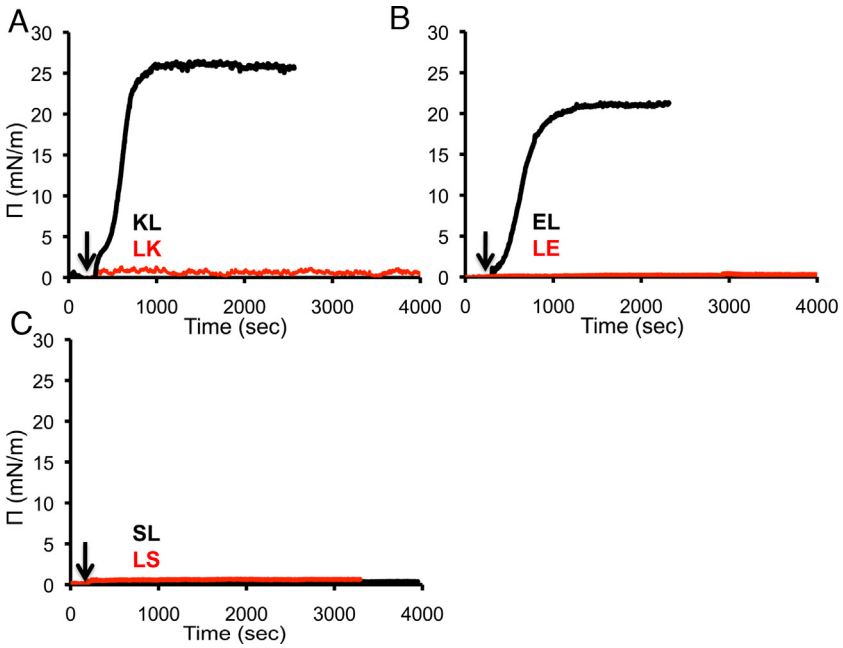

Fig. 2. Peptide adsorption into the air–water interface. Lateral surface pressure vs. time for the adsorption of KL and LK (A), EL and LE (B) and SL and LS peptides (C). Black lines: N-philic peptides. Red lines: C-philic peptides. Arrows: time of peptide injection. The peptide bulk concentration is 1.9 μM. The data shown is from one set of experiments where at least two replicates were performed. (For interpretation of the references to colour in this figure legend, the reader is referred to the web version of this article.)

3.5. Peptide–lipid interaction

From the characteristic differences in the surface behaviour of N-philic and C-philic peptides, we evaluated whether sequence inversion might also influence the interaction of these peptides with lipids. For this reason, we tested the ability of the peptides to penetrate POPC monolayers at a specific lateral packing (lateral surface pressure). In addition, we monitored tryptophan's proximity to POPC interfaces when NBD-labelled POPC liposomes were inoculated with the peptides.

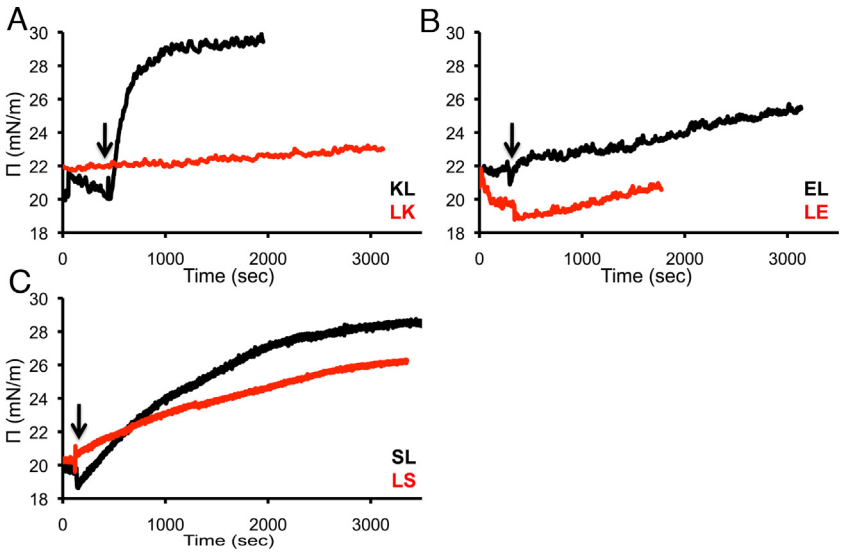

Fig. 3. Peptide penetration into the POPC monolayers at 20 mN/m. Lateral surface pressure vs. time for the penetration of KL and LK (A), EL and LE (B) and SL and LS peptides (C). Black lines: N-philic peptides. Red lines: C-philic peptides. Arrows: time of peptide injection. The peptide bulk concentration is 1.9 μM. The data shown is from one set of experiments where at least two replicates were performed. (For interpretation of the references to colour in this figure legend, the reader is referred to the web version of this article.)

3.6. Peptide penetration into lipid monolayers

Fig. 3 shows the penetration of N- and C-philic peptides into POPC monolayers packed at 20 mN/m. Again, differences between peptide isomers are clearly observed, with the N-philic charged peptides showing a higher capacity to penetrate the lipid monolayer than the C-philic retro-isomers. This difference is less evident for the neutral version of the peptides where, although SL has a higher propensity to penetrate the lipid monolayer than LS, LS is also able to penetrate the POPC monolayer, in contrast to the other C-philic peptides. It should be noted that neither LS nor SL peptides showed adsorption into the clean air–aqueous interface but they were able to penetrate POPC monolayers. This effect has been found for several amphipathic molecules and peptides. This is probably because lipid monolayers confer a more hydrophobic environment to the interface [32–34].

3.7. Tryptophan-NBD FRET

In order to evaluate whether peptides can interact with lipid bilayers, we monitored the FRET between the tryptophan residue present in the peptide sequence and a fluorescent lipid (NBD-PE) incorporated in the lipid bilayer of LUVs. As can be seen in Fig. 4, N-philic peptides again showed different behaviour to that of C-philic peptides. N-philic peptides presented a marked FRET signal after injection, but C-philic peptides did not induce an increase in NBD fluorescence. The lack of FRET signal does not rule out peptide binding to membranes. To assess whether or not there is binding of the C-philic peptides to POPC LUVs, we also performed flotation experiments (see Supplementary material, Fig. S5), which indicated that both types of peptides are bound to LUVs, which implies that the peptide orientation at the lipid interface, and therefore tryptophan's proximity to NBD, relies on the peptide sequence arrangement.

3.8. Peptide structure: ATR-FTIR of pure peptide films on diamond surface

FTIR of adsorbed proteins onto reflective surfaces is a powerful technique to determine the molecular secondary structure [35,36]. For this reason, we measured the IR absorption of pure peptide films onto the surface of a diamond crystal. We found that all the peptides adopted a mainly beta-sheet structure on this surface. Fig. 5 shows the ATR-FTIR absorption spectra of KL and LK peptides, where no significant differences are found between their curves. The results from the curve fitting are summarised in Table 3 for all peptides where the percentage contributions of each secondary structure are reported. This means that all the peptides may adopt a similar interfacial structure, emphasizing that the differences in observed surface behaviour between N- and C-philic peptides are not due to singular structural differences adopted by each type of molecule. Slight differences in the percentile contribution of the beta-sheet assignment are observed between peptides. As described for the fitting procedure, all the possible secondary structures were considered. For short-sequence peptides, the sensitivity of the band fitting is low, since a single amino-acid structural change will have a 10% impact on the overall structure. For this reason, we can confirm with this technique that the main structure of the peptides is beta-sheet but the differences observed between peptides in the amount of this structure probably fall within the deviation of the band assignment.

Table 3
Secondary structure analysis of N and C-philic peptides assessed by ATR-FTIR. The global percentage secondary structure composition of each ATR-FTIR spectrum for N and C-philic peptides is shown. Wave number (cm^{-1}) range considered for each assignment: 1918–1632 and 1689–1692, β-sheet; 1638–1645, random; 1648–1655, α-helix; 1660–1680, turns. The band assignment was performed for one set of experiments and two independent replicates were performed.

Assignments	Peptide					
	KL	LK	EL	LE	SL	LS
β-sheet	54	67	49	68	61	51
Random	18	14	16	8	19	17
α-Helix	14	11	20	14	9	17
Turn	14	8	15	10	11	15

4. Discussion

The biological activity of many proteins and peptides is through association/adsorption to cellular membranes. The sequence of the peptides or of the protein sections that directly interact with the lipids has to have a perfect design. The aim of this work is to provide

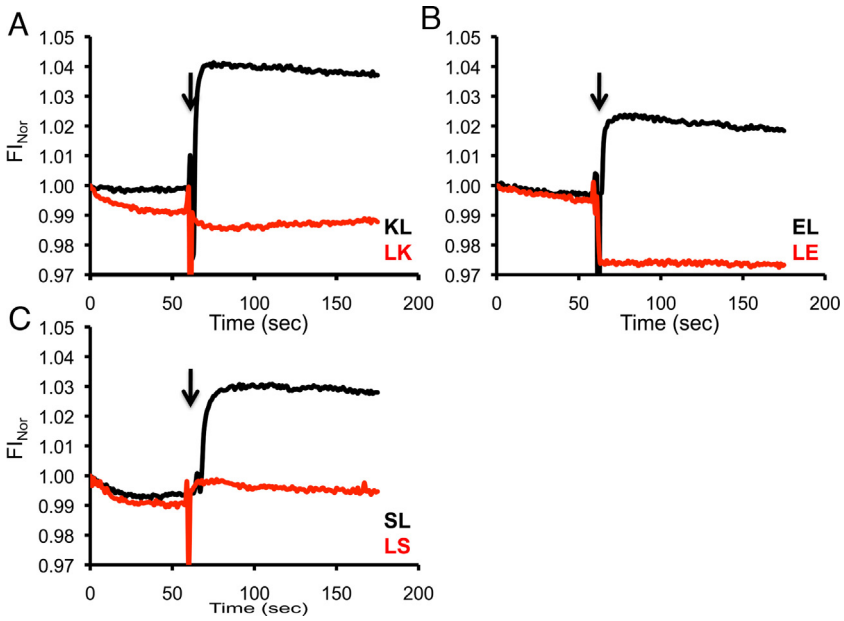

Fig. 4. Tryptophan-NBD fluorescence energy transfer. Normalised NBD-PE fluorescence intensity vs. time before and after injection of KL and LK (A), EL and LE (B) and SL and LS (C) peptides into a cuvette with 1.5 mM POPC LUVs containing 1% of the NBD-PE lipid. Black lines: N-philic peptides. Red lines: C-philic peptides. Arrows: time of peptide injection. Peptide final concentration: 4 μM. λ_{ex}: 280 nm; λ_{em}: 536 nm. Note in B a slight decrease of signal after injection probably due to an artefact after peptide addition. The data shown is from one set of experiments where at least two replicates were performed. (For interpretation of the references to colour in this figure legend, the reader is referred to the web version of this article.)

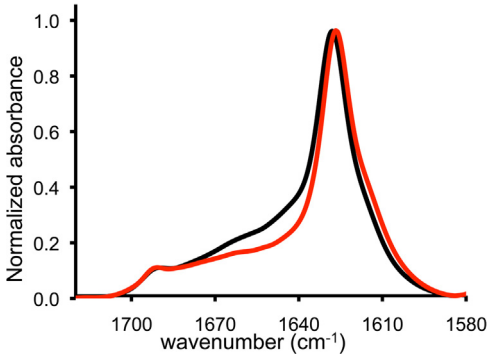

Fig. 5. Secondary structure of N-philic and C-philic peptides. ATR-FTIR absorption spectra of KL (black) and LK (red) adsorbed onto a diamond surface. Similar spectra were found for EL, SL, LE and LS (not shown). The data shown is from one set of experiments where at least two independent replicates were performed. (For interpretation of the references to colour in this figure legend, the reader is referred to the web version of this article.)

further information on the propensity and interfacial stability of a set of peptides in which we control not only the orientation of the hydrophilic/hydrophobic residues along the peptide sequence, but also the chemistry of the hydrophilic amino-acids. We found that the peptides we tested mainly adopted a beta-sheet structure when adsorbed to a diamond surface. This structure correlates with the hexapeptide $AcWL_5$, a molecule that has a remarkable ability to assemble reversibly and spontaneously into β-sheets on lipid membranes [15,37] and resembles the hydrophobic section of the peptides studied in the present work. In addition, previous reports from other laboratories and from our own work demonstrated that peptides that adopt this conformation at the air–aqueous interface have high stability against lateral compression [20,38].

We observed a sharply defined difference in lateral stability and interfacial affinity. N-philic peptides form insoluble films that collapse at higher pressures than those composed by C-philic peptides, and those N-philic peptides with charged residues are more prone to self-incorporate into the clean air–water interface and into a lipid monolayer. The higher stability of the N-philic peptide films was further confirmed by in silico molecular dynamic simulations (Supplementary material), reinforcing the experimental data and showing the importance of a specific peptide sequence arrangement for a given surface stability. In addition, the rheological properties of the insoluble films developed by these peptides at the air–water interface were very similar, with all of them being mainly elastic and with marked shear contributions. These results (together with the low diffusion of micrometre-sized beads) match what is found for the amyloid peptides Aβ 1-40 and 1-42, whose high shear modulus is interpreted as a consequence of the formation of a beta-sheet array at the air–water interface (Caruso et al., unpublished results). It is also remarkable that there is an effect of the sequence inversion, since, within N-philic peptides, shear elasticity was much higher for the charged peptides. But the peptide design not only gives these features to the pure peptide monolayers but is also important for the interaction with the zwitterionic lipid POPC, in which the N-philic configuration (which resembles signal sequence peptides) increases the capacity to penetrate monolayers of this lipid and also to position the W residue closer to the polar head of the lipids.

5. Conclusions

Our findings are compelling in terms of how the peptide primary structure plays an essential role to dictate specific surface activity for molecules that have a similar secondary structure and identical hydrophobicity. Protein transport across membranes, peptide activity on bilayers and drug-delivery mediated by small proteins are fascinating topics for biophysicists trying to understand, at the molecular level, how these phenomena occur. All these properties may be modulated by the primary, and the consequent secondary, structure of the proteins. Peptide sequence inversion (retro-isomers) has been studied for over 60 years, trying to understand its effect on the biological activity of peptides. One of the earliest examples was the loss of activity for the retro-isomer of the vasodilator, bradykinin [39]. Another interesting

example is the effect of sequence inversion of the membrane-interacting cecropin–melittin peptide hybrids [40]. These chimeric peptides have been developed in order to increase their bacterial toxicity, as they are more potent than the normal antimicrobial peptide (cecropin) [41]. In principle, retro-isomerization of these cecropin–melittin hybrids would not alter the antimicrobial effect of the peptides, but some types of cells that were killed by the normal peptides were now resistant to the retro-isomer [41]. Another interesting study demonstrates that sequence inversion of the ALPS (amphipathic lipid-packing sensor) motif of $GMAP_N$ does not affect the capacity of the protein to accumulate early secretory pathway vesicles [42]. From these data, the biological effect of retro-isomeric molecules when interacting with membranes is still not clear. For some peptides, it has a strong effect on specific membranes but others remain invariable [43].

Here we provide a small, but strong, piece of evidence of how proteins could completely change their interfacial behaviour by fine-tuning of the amino acid arrangement, despite their having the same global physical–chemical properties. This is reflected in the way in which SSPs are able to resist high-lateral pressures when inserted into the lipid membrane [20] given by the first half of the sequence that resembles the N-philic configuration.

Acknowledgements

This work was supported in part by grants from Agencia FONCYT Préstamo BID 2012 PICT 1377 to E.E.A, Préstamo BID 2011 PICT 1784 to G.D.F, CONICET, SECyT-UNC and the bilateral CONICET-FNRS (year 2012) grant. We especially thank Jean-Marie Ruysschaert (Centre de Biologie Structurale et de Bioinformatique, Université Libre de Bruxelles, Belgium) and our colleagues at Centro de Investigaciones en Química Biológica de Córdoba for many helpful discussions and Joss Heywood for careful reading of the manuscript. E.E.A is a Career Member of Consejo Nacional de Investigaciones Científicas y Técnicas (CONICET). VR is Senior Research Associate for the F.R.S-FNRS (Belgium).

Appendix A. Supplementary data

Supplementary data associated with this article can be found, in the online version, at http://dx.doi.org/10.1016/j.colsurfb.2015.12.008.

References

[1] S.H. White, Membrane protein insertion: the biology–physics nexus, J. Gen. Physiol. 129 (2007) 363–369.
[2] S.J. Dunne, R.B. Cornell, J.E. Johnson, N.R. Glover, A.S. Tracey, Structure of the membrane binding domain of CTP: phosphocholine cytidylyltransferase, Biochemistry 35 (1996) 11975–11984.
[3] B. Antonny, S. Beraud-Dufour, P. Chardin, M. Chabre, N-terminal hydrophobic residues of the G-protein ADP-ribosylation factor-1 insert into membrane phospholipids upon GDP to GTP exchange, Biochemistry 36 (1997) 4675–4684.
[4] C.C. Jao, A. Der-Sarkissian, J. Chen, R. Langen, Structure of membrane-bound alpha-synuclein studied by site-directed spin labeling, Proc. Natl. Acad. Sci. U. S. A. 101 (2004) 8331–8336.
[5] M. Dathe, T. Wieprecht, Structural features of helical antimicrobial peptides: their potential to modulate activity on model membranes and biological cells, Biochim. Biophys. Acta 1462 (1999) 71–87.
[6] Y. Shai, Mode of action of membrane active antimicrobial peptides, Biopolymers 66 (2002) 236–248.
[7] E.E. Ambroggio, F. Separovic, J.H. Bowie, G.D. Fidelio, L.A. Bagatolli, Direct visualization of membrane leakage induced by the antibiotic peptides: maculatin, citropin, and aurein, Biophys. J. 89 (2005) 1874–1881.
[8] G. Thakur, C. Pao, M. Micic, S. Johnson, R.M. Leblanc, Surface chemistry of lipid raft and amyloid Abeta (1–40) Langmuir monolayer, Colloids Surf B Biointerfaces 87 (2011) 369–377.
[9] G. Thakur, M. Micic, R.M. Leblanc, Surface chemistry of Alzheimer's disease: a Langmuir monolayer approach, Colloids Surf. B Biointerfaces 74 (2009) 436–456.
[10] M.C. Lee, L. Orci, S. Hamamoto, E. Futai, M. Ravazzola, R. Schekman, Sar1p N-terminal helix initiates membrane curvature and completes the fission of a COPII vesicle, Cell 122 (2005) 605–617.
[11] M.G. Ford, I.G. Mills, B.J. Peter, Y. Vallis, G.J. Praefcke, P.R. Evans, H.T. McMahon, Curvature of clathrin-coated pits driven by epsin, Nature 419 (2002) 361–366.
[12] K. Farsad, N. Ringstad, K. Takei, S.R. Floyd, K. Rose, P. De Camilli, Generation of high curvature membranes mediated by direct endophilin bilayer interactions, J. Cell Biol. 155 (2001) 193–200.
[13] J. Bigay, J.F. Casella, G. Drin, B. Mesmin, B. Antonny, ArfGAP1 responds to membrane curvature through the folding of a lipid packing sensor motif, EMBO J. 24 (2005) 2244–2253.
[14] E. Ambroggio, B. Sorre, P. Bassereau, B. Goud, J.B. Manneville, B. Antonny, ArfGAP1 generates an Arf1 gradient on continuous lipid membranes displaying flat and curved regions, EMBO J. 29 (2010) 292–303.
[15] W.C. Wimley, S.H. White, Reversible unfolding of beta-sheets in membranes: a calorimetric study, J. Mol. Biol. 342 (2004) 703–711.
[16] G. Von Heijne, Membrane protein assembly in vivo, Adv. Protein Chem. 63 (2003) 1–18.
[17] G. von Heijne, Transcending the impenetrable: how proteins come to terms with membranes, Biochim. Biophys. Acta 947 (1988) 307–333.
[18] T.A. Rapoport, Protein translocation across the eukaryotic endoplasmic reticulum and bacterial plasma membranes, Nature 450 (2007) 663–669.
[19] A. Weihofen, K. Binns, M.K. Lemberg, K. Ashman, B. Martoglio, Identification of signal peptide peptidase, a presenilin-type aspartic protease, Science 296 (2002) 2215–2218.
[20] E.E. Ambroggio, G.D. Fidelio, Lipid-like behavior of signal sequence peptides at air–water interface, Biochim. Biophys. Acta 1828 (2013) 708–714.
[21] M. Chorev, M. Goodman, Recent developments in retro peptides and proteins—an ongoing topochemical exploration, Trends Biotechnol. 13 (1995) 438–445.
[22] N. Wilke, Chapter two—lipid monolayers at the air–water interface: a tool for understanding electrostatic interactions and rheology in biomembranes, I. Ale≈◦, V.K. Chandrashekhar (Eds.), Advances in Planar Lipid Bilayers and Liposomes, Academic Press, 2014, pp. 51-81.
[23] N. Wilke, F. Vega Mercado, B. Maggio, Rheological properties of a two phase lipid monolayer at the air/water interface: effect of the composition of the mixture, Langmuir 26 (2010) 11050–11059.
[24] P. Cicuta, E.M. Terentjev, Viscoelasticity of a protein monolayer from anisotropic surface pressure measurements, Eur. Phys. J. E Soft Matter 16 (2005) 147–158.
[25] J.T. Petkov, T.D. Gurkov, B.E. Campbell, R.P. Borwankar, Dilatational and shear elasticity of gel-like protein layers on air/water interface, Langmuir 16 (2000) 3703–3711.
[26] L.D. Mayer, M.J. Hope, P.R. Cullis, Vesicles of variable sizes produced by a rapid extrusion procedure, Biochim. Biophys. Acta 858 (1986) 161–168.
[27] A. Clausell, F. Rabanal, M. Garcia-Subirats, M. Asuncion Alsina, Y. Cajal, Membrane association and contact formation by a synthetic analogue of polymyxin B and its fluorescent derivatives, J. Phys. Chem. B 110 (2006) 4465–4471.
[28] E. Goormaghtigh, V. Cabiaux, J.M. Ruysschaert, Determination of soluble and membrane protein structure by Fourier transform infrared spectroscopy. I. Assignments and model compounds, Subcell. Biochem. 23 (1994) 329–362.
[29] G.L. Gaines, Insoluble Monolayers at Liquid–Gas Interfaces, Interscience, New York, 1966.
[30] M. Hackel, H.J. Hinz, G.R. Hedwig, Partial molar volumes of proteins: amino acid side-chain contributions derived from the partial molar volumes of some tripeptides over the temperature range 10–90 ◦C, Biophys. Chem. 82 (1999) 35–50.
[31] F. Monroy, F. Ortega, R.G. Rubio, H. Ritacco, D. Langevin, Surface rheology of two-dimensional percolating networks: Langmuir films of polymer pancakes, Phys. Rev. Lett. 95 (2005) 056103.
[32] M.E. Mariani, R.R. Madoery, G.D. Fidelio, Auxins action on glycine max secretory phospholipase A2 is mediated by the interfacial properties imposed by the phytohormones, Chem. Phys. Lipids 189 (2015) 1–6.
[33] B.A. Isse, P. Yunes Quartino, G.D. Fidelio, R.N. Farias, Thyroid hormones–membrane interaction: reversible association of hormones with organized phospholipids with changes in fluidity and dipole potential, Chem. Phys. Lipids 175–176 (2013) 131–137.
[34] M. Gonzalez, N. Lezcano, M.E. Celis, G.D. Fidelio, Interaction of alpha-MSH and substance P with interfaces containing gangliosides, Peptides 17 (1996) 269–274.
[35] R. Sarroukh, E. Goormaghtigh, J.M. Ruysschaert, V. Raussens, ATR-FTIR: a rejuvenated tool to investigate amyloid proteins, Biochim. Biophys. Acta 1828 (2013) 2328–2338.
[36] Y. Shai, ATR-FTIR studies in pore forming and membrane induced fusion peptides, Biochim. Biophys. Acta 1828 (2013) 2306–2313.
[37] W.C. Wimley, K. Hristova, A.S. Ladokhin, L. Silvestro, P.H. Axelsen, S.H. White, Folding of beta-sheet membrane proteins: a hydrophobic hexapeptide model, J. Mol. Biol. 277 (1998) 1091–1110.
[38] R. Maget-Dana, D. Lelievre, A. Brack, Surface active properties of amphiphilic sequential isopeptides: comparison between alpha-helical and beta-sheet conformations, Biopolymers 49 (1999) 415–423.
[39] M. Bodanszky, M.A. Ondetti, J.T. Sheehan, S. Lande, Synthetic peptides related to bradykinin, Ann. N. Y. Acad. Sci. 104 (1963) 24–34.

[40] D. Wade, A. Boman, B. Wåhlin, C.M. Drain, D. Andreu, H.G. Boman, R.B. Merrifield, All-D amino acid-containing channel-forming antibiotic peptides, Proc. Natl. Acad. Sci. U. S. A. 87 (1990) 4761–4765.
[41] R.B. Merrifield, P. Juvvadi, D. Andreu, J. Ubach, A. Boman, H.G. Boman, Retro and retroenantio analogs of cecropin–melittin hybrids, Proc. Natl. Acad. Sci. U. S. A. 92 (1995) 3449–3453.
[42] I.M. Pranke, V. Morello, J. Bigay, K. Gibson, J.-M. Verbavatz, B. Antonny, C.L. Jackson, α-Synuclein and ALPS motifs are membrane curvature sensors whose contrasting chemistry mediates selective vesicle binding, J. Cell Biol. 194 (2011) 89–103.
[43] P.M. Fischer, The design, synthesis and application of stereochemical and directional peptide isomers: a critical review, Curr. Protein Pept. Sci. 4 (2003) 339–356.